

## Surfaces, Interfaces, and Applications

**Rapid on-chip assembly of niosomes: batch versus continuous flow reactors**

Sara Garcia-Salinas, Erico Himawan, Gracia Mendoza, Manuel Arruebo, and Victor Sebastian Cabeza

ACS Appl. Mater. Interfaces, **Just Accepted Manuscript** • DOI: 10.1021/acsami.8b02994 • Publication Date (Web): 16 May 2018Downloaded from <http://pubs.acs.org> on May 17, 2018**Just Accepted**

“Just Accepted” manuscripts have been peer-reviewed and accepted for publication. They are posted online prior to technical editing, formatting for publication and author proofing. The American Chemical Society provides “Just Accepted” as a service to the research community to expedite the dissemination of scientific material as soon as possible after acceptance. “Just Accepted” manuscripts appear in full in PDF format accompanied by an HTML abstract. “Just Accepted” manuscripts have been fully peer reviewed, but should not be considered the official version of record. They are citable by the Digital Object Identifier (DOI®). “Just Accepted” is an optional service offered to authors. Therefore, the “Just Accepted” Web site may not include all articles that will be published in the journal. After a manuscript is technically edited and formatted, it will be removed from the “Just Accepted” Web site and published as an ASAP article. Note that technical editing may introduce minor changes to the manuscript text and/or graphics which could affect content, and all legal disclaimers and ethical guidelines that apply to the journal pertain. ACS cannot be held responsible for errors or consequences arising from the use of information contained in these “Just Accepted” manuscripts.

# Rapid on-chip assembly of niosomes: batch versus continuous flow reactors

Sara Garcia-Salinas<sup>1,2,3</sup>, Erico Himawan<sup>1,2</sup>, Gracia Mendoza<sup>1,2</sup>, Manuel Arruebo<sup>1,2,3\*</sup> and Victor Sebastian<sup>1,2,3\*</sup>

<sup>1</sup>Department of Chemical Engineering and Environmental Technology and Institute of Nanoscience of Aragon (INA), University of Zaragoza (Spain)

<sup>2</sup>Aragon Health Research Institute (IIS Aragón), 50009 Zaragoza, Spain

<sup>3</sup>Networking Research Center on Bioengineering, Biomaterials and Nanomedicine, CIBER-BBN, 28029 Madrid (Spain)

**KEYWORDS.** *Niosomes, microfluidics, microchannel emulsification, multilamellar vesicles, non-ionic surfactant vesicles*

**ABSTRACT:** The large-scale continuous production of niosomes remains challenging. The inherent drawbacks of batch processes such as large particle polydispersity and reduced batch-to-batch reproducibility are here overcome by using commercially available microfluidic reactors. Compared to the traditional batch-based film hydration method, herein, we demonstrate that it is possible to carry out the homogeneous, large-scale (up to 120mg/min) production of niosomes using two different synthesis techniques (the thin film hydration method and the emulsification technique). Niosomes particle size can be controlled depending on the need by varying the synthesis temperature. The high cytocompatibility of the resulting niosomes was also demonstrated in this work on three different somatic cell lines. For the first time, the structure of the niosome multi-lamellar shell was also elucidated using high-resolution transmission electron microscopy (HR-STEM) as well as their colloidal stability over time (6 weeks) under different storage conditions. The morphology of cryo-protected or as-made niosomes was also evaluated by HR-STEM after freeze-drying. Finally, the dual ability of those synthetic, non-ionic, surfactant based vesicles to carry both hydrophilic and hydrophobic molecules was also here demonstrated by using laser scanning confocal microscopy.

## INTRODUCTION

The production of organic nanoparticles (NPs) has not been as extensively studied as the production of inorganic ones,<sup>1</sup> which is surprising considering their extended use in the fields of pharmaceuticals<sup>2</sup>, nanomedicine<sup>3</sup> and food industry.<sup>4</sup> The most studied production approaches are based on emulsion-based and nanoprecipitation methods. Both approaches require achieving a high mixing performance in order to control the NP size and the amount of active principle loaded. In the emulsion-based methods the emulsion is an intermediate stage where an immiscible organic phase is confined in small droplets, which act as a template for the organic NP formation. The organic NPs are finally produced by separating the organic solvent via evaporation<sup>5</sup> or by diffusion processes with the consequent polymer precipitation.<sup>1,6</sup> Nanoprecipitation, on the other hand, relies on the creation of a supersaturated solution using miscible solvents, by means of a temperature change<sup>7</sup> or by solvent displacement,<sup>8</sup> which ultimately leads to the formation of an insoluble precipitate composed of dispersed organic NPs.<sup>1</sup>

Organic NPs enhance the solubility of poorly aqueous soluble drugs/biomolecules and enable to control their release by means of biological or physical degradation. Consequently, special production techniques are required in order to disperse non-soluble organic molecules into water, maintain the dispersion stable for a certain period of time, control the size and functionalize the surface of the resulting organic NPs to minimize aggregation and opsonization during their potential par-

enteral administration.<sup>9</sup> These strict requirements pose serious challenges to their mass production, including limited batch-to-batch reproducibility and controllability, in terms of morphological and physicochemical properties.<sup>10,11</sup> A wide variety of multistep batch laboratory procedures are not amenable to large-scale production because they require time consuming post-production steps (e.g., density-gradient centrifugation, size-exclusion chromatography, ion-exchange chromatography, electrophoresis, selective precipitation, preferential solubility, membrane filtration, extraction, etc.) to improve size uniformity and maintain a high standard. As a result, there is often a balance between maintaining the ability to control the desired nanoscale features and achieving high production throughput.<sup>11</sup> Consequently, the development of new technologies tackling some of these challenges could significantly accelerate the clinical translation of organic NPs.

Niosomes are the synthetic, non-ionic, counterparts of liposomes, formed by self-assembly of non-ionic surfactants. The self-assembly of amphiphilic surfactants into closed bilayers to form niosomes is not spontaneous and requires some input of well-spatially distributed energy such as ultrasound, heat or mechanical shaking. In addition, niosomes are only thermodynamically stable in presence of appropriate mixtures of surfactants and surface charge inducing agents.<sup>12</sup> The basic components of niosomes include non-ionic surfactants, a hydration medium, charged inducing agents and steroids such as cholesterol. Charged inducing agents, either positive or negative, are used for preventing the aggregation of niosomes since it is

well considered that zeta ( $\zeta$ )-potentials over  $|30|$  mV are necessary for full electrostatic colloidal stabilization.<sup>12</sup> Charge inducing agents act by preventing the fusion of niosomes due to repulsive forces of the same charge. Cholesterol reduces the temperature of the vesicular gel to liquid crystal phase transition and decreases the overall Hydrophile-Lipophile Balance (HLB) value of the surfactant mixture.<sup>13</sup> In addition, cholesterol improves the cohesion of the niosomal membrane to decrease its permeability and influences the physical properties and structure of niosomes because several surfactants form vesicles only after cholesterol addition.<sup>14</sup> However, cholesterol decreases the entrapment volume during formulation, affecting the loading efficiency.<sup>15</sup>

Since the initial development of niosomes by L'Oreal for cosmetic applications in the late 1970s, they have been evaluated in therapeutic applications due to their ability to reduce systemic toxicity and minimize clearance. Niosomes are suitable for the delivery of numerous pharmacological and diagnostic agents via different routes<sup>2, 12, 16-18</sup>: 1) Dermal and transdermal; 2) Ocular; 3) Oral; 4) Pulmonary and 5) Parenteral. Taking into account the enormous prospective of niosomes in drug delivery and diagnostics, an increasing research interest is arising in stable niosomal formulations because niosomes are able to overcome some disadvantages associated with liposomes<sup>12</sup>: 1) surfactants are easily derivatized 2) give a higher versatility to control the vesicular structure 3) high stability towards oxidative degradation and 4) they have lower costs than phospholipids.

Niosomes can be prepared as unilamellar or multilamellar vesicles, where hydrophilic molecules can be encapsulated within their aqueous core, while hydrophobic molecules can be partitioned into their lamellar structure. The standard bulk methods for niosomal formulation can be summarized as<sup>12</sup>: thin film hydration method (FHM), the organic solvent injection method, the reverse phase evaporation method and the gas-bubble method. However, conventional bulk methods for producing niosomes suffer from the poor control over the chemical and mechanical environment.<sup>1</sup> The lack of control in mixing conditions often leads to large niosomes with high size polydispersity, thus affecting the envisaged niosome application. Post-processing steps such as extrusion or sonication are then required to reduce and homogenize their size.

Microfluidic technology faces those previous limitations and leads to improve the mean size and size distributions of niosomes by taking advantage of the rapid and controlled mixing of reagents. Microfluidic reactors offer a plethora of potential advantages for the production of NPs<sup>19</sup> and transform current classical batch technologies for the production of NPs into continuous well-controlled microfluidic process: 1) Accurate control and manipulation of fluids and fluid interfaces with a homogenous reaction environment; 2) Rapid and uniform heat and mass transfer; 3) In-situ monitoring of the progress of NPs formation; d) Excellent reproducibility; e) Rapid screening of synthesis parameters and f) High-throughput continuous production and limited undesirable by-product formation. Although the production of niosomes in batch-type reactors has been widely studied<sup>16, 17, 20</sup>, the translation to a controlled and continuous process has been scarcely studied.

Lo et al.<sup>21</sup> reported for the first time the continuous production of niosomes by a microfluidic hydrodynamic flow focusing system fabricated in Polydimethylsiloxane (PDMS) and silicon. Controlling the diffusive mixing time was crucial to

promote the homogenous assembly of niosomes with smaller sizes and more monodisperse in size distribution than the ones retrieved from conventional bulk methods. The synthesis procedure described was based on the thin film hydration method. In this method, the surfactants and additives are dissolved in an organic solvent in a round-bottom flask.<sup>22</sup> The thin film is formed on the inside wall of the flask by removing the organic solvent. Finally, an aqueous/alcoholic solution is added and the dry film is hydrated above the transition temperature of the surfactant to promote the formation of niosomes.<sup>22</sup> According to Lo et al.<sup>21</sup> it was first required the production of a Span-cholesterol-DCP (dicetyl phosphate) dry film and the subsequent resolubilization in isopropyl alcohol (IPA). The niosome assembly was promoted by the mixing of two miscible fluids IPA and a hydration buffer. The results achieved were remarkable, but the dry-film preparation is a time consuming stage that hampers the high-throughput production of niosomes when using a continuous approach. This reported method has been considered recently as an inspiration for the production of non-ionic surfactant vesicles by a hydrodynamic microflow system,<sup>23</sup> but using lipids instead of the well-studied surfactants used for niosome preparation (Span, Tween or Brij).<sup>22</sup>

In this study, we present a new method of niosome self-assembly by microfluidic hydrodynamic focusing without the need of a size reduction step, as required in the conventional methods. The microfluidic system is a commercial micromixer that can enable an easy reproduction of the reported results. This fact is of enormous importance because the majority of microfluidic systems reported in organic nanomaterial synthesis are custom made microfabricated silicon/PDMS-based reactors with a limited access by non-microfluidic skilled users. The novelty of this work is based on the production of niosomes in continuous flow without the need of a thin film formation and by using an emulsification process. This strategy exerts the advantage of reducing the timeline reported by Lo et al.<sup>21</sup>, increasing considerably the production throughput and avoids the use of a toxic solvent during the thin film evaporation. This study has selected sorbitan esters (Span) as non-ionic surfactants because they are FDA approved additives for use in food processing and pharmaceuticals<sup>21</sup>. The proposed method has been benchmarked with the thin film formation technique assisted by microfluidics and by using batch-type reactors. Niosomes have been characterized by the first time using high-resolution electron microscopy, obtaining excellent information about the bilayers structure. Confocal microscopy was carried out to verify that dual hydrophilic and hydrophobic molecules could be loaded in niosomes. *In vitro* cytotoxicity experiments were subsequently performed to evaluate the subcytotoxic dose of the produced niosomes on different cell lines.

## EXPERIMENTAL SECTION

**Reactants.** Cholesterol, Sorbitan monolaurate-Span20, Dicyetyl phosphate (DCP), Nile Red, Fluorescein, Phosphotungstic acid, 2-propanol (IPA) and Ethyl acetate were purchased from Sigma-Aldrich (St. Louis, MO) and used as received.

**Film hydration method in batch type reactors.** Niosome formation was carried out using a modification of the procedure reported by Paolino et al.<sup>24</sup> as here briefly described (Figure 1-a). A mixture of 52 mg of Span20, 58 mg of Cholesterol and 8.6mg of DCP (47.5:47.5:5 molar ratio) was dis-

solved in 400  $\mu\text{L}$  of ethyl acetate and mixed at 60°C in a glass scintillation vial during 5 min. The organic solvent was then evaporated under  $\text{N}_2$  reflux during 4 h to obtain a dry film on the bottom of the scintillation vial. After that, sample was left overnight in a desiccator to achieve the total organic solvent evaporation. After 12 h of drying, the dry film was resolubilized with 400  $\mu\text{L}$  of IPA at 60°C during 5 min. Niosomal suspension was mixed with 20 mL of milli-Q water at 35°C and subjected to ten cycles of sonication during 1 min, each using a Branson Digital Sonifier (Model 450) operating at 30% of amplitude output following a 0.5 min pause between each sonication. The resulting homogeneous emulsion was then kept under mechanical stirring during 1h to allow the evaporation of the organic solvent present in the sample.

**Film hydration method in microfluidic reactors.** The dry film was prepared as it was previously described in the batch type procedure. 400  $\mu\text{L}$  of IPA were added to the dry film to obtain a complete resolubilized solution. The organic phase was loaded in a syringe and injected with a flow rate of 15.7  $\mu\text{L/s}$ . The aqueous phase was injected with a flow rate of 768.3  $\mu\text{L/s}$ . The micromixer promoted the phase multilamination and then, the subsequent niosome self-assembly (Figure 1-b).

**Emulsification method in microfluidic reactors.** A mixture of 52 mg of Span20, 58 mg of Cholesterol and 8.6 mg of DCP (47.5:47.5:5 molar ratio) was dissolved in 400  $\mu\text{L}$  of ethyl acetate and mechanically mixed at 60°C in a water bath during 5 min. The prepared solution was loaded in a syringe and injected in the interdigital micromixer with a 15.7  $\mu\text{L/s}$  flow rate. The temperature in the syringe was kept constant to prevent reagents precipitation. An additional stream of Milli-Q water at different temperatures (25 °C-55 °C) was injected in the micromixer with a flow rate of 768.3  $\mu\text{L/s}$  (Figure 1-b). The outlet stream was collected in a glass vial and kept under mechanical stirring during 15 minutes to allow the evaporation of the organic solvent.

The hydrophilic/hydrophobic loading potential of niosomes was studied by loading two types of fluorescent dyes (Figure 1-c): 1) Hydrophobic-Red Nile was dispersed in the organic stream, 0.1 mg/mL. 2) Hydrophilic, sodium fluorescein was added to the aqueous stream 0.1 mg/mL.

**Microfluidic reactors.** Niosomes were prepared using a Polyether ether ketone (PEEK) slit interdigital micromixer with an inner volume of 8  $\mu\text{L}$  (Micro4Industries GmbH, Mainz, Germany) interfaced with Polytetrafluoroethylene (PTFE) tubing (OD = 1/16", ID = 1 mm) (Figure 1-b). The slit-interdigital micromixer follows the principle of producing thin liquid lamellae, guiding the inlet streams in contact through a flow-through-chamber. The organic and aqueous phase streams were introduced in the micromixer by means of syringe pumps (Harvard Apparatus PHD Ultra™ CP 4400), ensuring a good control of the flow rates with very low pulsation. The injected streams were split into 16 substreams of 45  $\mu\text{m}$  width each. Substreams were later on recombined to increase the contact surface between the two immiscible phases to produce the emulsification process and the assembly of the niosomes.

#### Niosomes characterization.

**Dynamic light scattering.** The hydrodynamic diameter and size distribution of the resulting niosomes were determined by dynamic light scattering measurements using a Brookhaven 90

Plus (Holtville, NY) equipment. 100  $\mu\text{L}$  of the niosomal suspension were suspended in 1.5mL of distilled water and sonicated before measurements. Each sample was measured three times to obtain a significant value.

**Zeta potential measurements.** The zeta potential of niosomes was directly related to their surface charge density and was measured by using a Brookhaven 90 Plus equipment. Zeta potential values were determined using 100  $\mu\text{L}$  of the niosome sample and adding 1.0 mL of 1mM KCl at pH 7.4. Three repeated measurements of the Z potential were performed for each individual experiment.

**Morphological studies.** The morphological characterization of the resulting niosomes was performed at the LMA-INA facilities in a Transmission Electron Microscope TEM (TECNAI FEI T20) operating at an acceleration voltage 200 kV with a LaB6 electron source fitted with a "SuperTwin®" objective lens allowing a point-to-point resolution of 2.4 Å. Aberration corrected scanning transmission electron microscopy (Cs-corrected STEM) images were acquired using a high angle annular dark field detector in a FEI XFEI TITAN electron microscope operated at 300 kV equipped with a CETCOR Cs-probe corrector from CEOS. The niosome samples were stained with 7% (w/v) phosphotungstic acid as a negative contrast to facilitate bilayer observation. Particle size histograms were obtained according to best practices in determination of nanoparticle size distribution<sup>25</sup>. Confocal microscopy was carried out to verify the hydrophilic and hydrophobic molecule loading in niosomes. A drop of the produced emulsion of niosomes was mounted on microscopy slides and visualized by confocal microscopy (Leica TCS SP2 Laser Scanning Confocal Microscope, Microscopy Unit, CIBA, IIS Aragon, Spain). Empty control samples were also tested to dismiss sample autofluorescence.

#### Biocompatibility studies.

**Cell cultures.** Fibroblasts, macrophages and keratinocytes were used as cell models to test the cytotoxicity of the resulting niosomes. Human dermal fibroblasts were purchased from Lonza (Belgium), THP1 human monocytes were obtained from the American Type Culture Collection (USA) and human epidermal keratinocytes (HaCat) were kindly donated by Dr. Pilar Martin-Duque.

Fibroblasts and HaCaT were grown in high-glucose DMEM (DMEM w/stable glutamine; Biowest, France) supplemented with 10% fetal bovine serum (FBS; Gibco, UK), penicillin/streptomycin (100 U/100  $\mu\text{g/mL}$ ; Lonza, Belgium), and amphotericin B (1.5  $\mu\text{g/mL}$ ; Lonza, Belgium). Monocytes were cultured in RPMI 1640 (RPMI 1640 w/stable glutamine; Biowest, France) supplemented with 10% FBS, 1% HEPES, 1% nonessential amino acids, 0.1% 2-mercaptoethanol, 1% sodium pyruvate 100mM, penicillin/streptomycin (100 U/100  $\mu\text{g/mL}$ ), and amphotericin B (1.5  $\mu\text{g/mL}$ ), all purchased from Gibco (UK). Macrophages were obtained by the *in vitro* differentiation of monocytes by adding 1  $\mu\text{M}$  phorbol 12-myristate 13-acetate (PMA) (Sigma-Aldrich, USA) to the cell culture. All cell types were grown in humidified atmosphere at 37°C and 5%  $\text{CO}_2$ .

**Cell cytotoxicity.** The cytotoxicity of niosomes in the cellular metabolism was studied by the Alamar Blue assay (Invitrogen, US). Fibroblasts, macrophages and keratinocytes were seeded in a 96-well plate and incubated with 0.01- 0.4 mg/mL of niosomal dispersions in water for 24h. Alamar Blue was then added (10%) and incubated for 4h. If the metabolism of

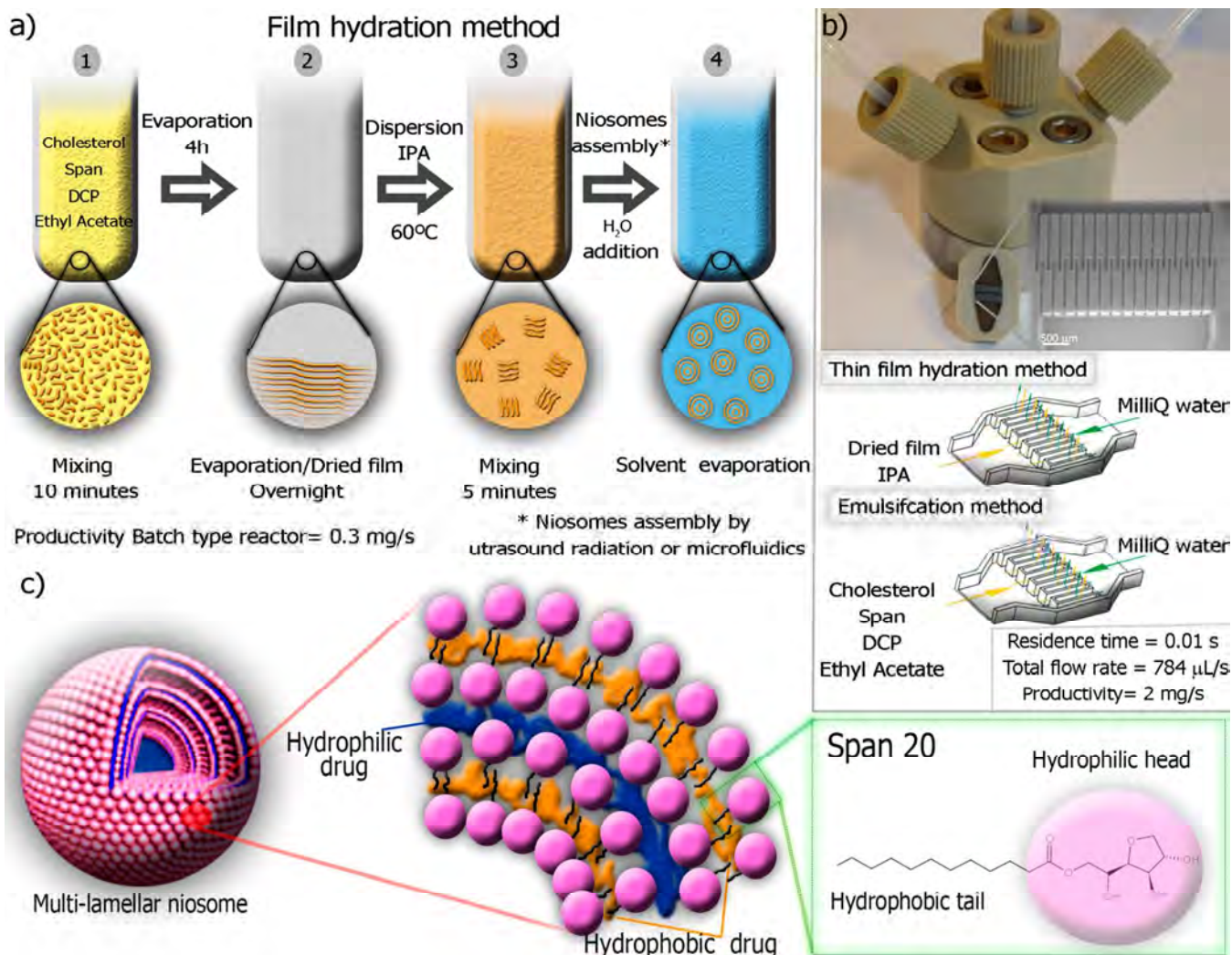


**Figure 1.-** a) Scheme of niosome synthesis by the thin film hydration method: 1) Mixing of niosome reagents, 2) Dry film formation, 3) Dry film dispersion and 4) Niosomes formation by solvent evaporation. b) Slit micromixer selected to produce niosomes in continuous fashion either by the film hydration method or by emulsification. c) Scheme of a multilamellar niosome and hydrophilic/hydrophobic loading scenario.

cells were active, the dye would change to a fluorescent compound which was read in a microplate reader (Multimode Synergy HT Microplate Reader; Biotek, US) at 535/591 nm ex/em. Cell viability was determined by interpolation of the emission data obtained from the treated samples and samples without nanoparticles (considered as the 100% of viability).

**Statistical analysis.** Statistical analysis was carried out using GraphPad Prism 7 for Windows (GraphPad Software, La Jolla, CA, USA). Three replicates for each experiment were performed and the results were analyzed as mean  $\pm$  standard deviation. A  $p$  value  $\leq 0.05$  was considered as significant,  $p < 0.01$  highly significant. Two-way ANOVA analysis was used for multiple comparisons using Dunnett statistical hypothesis test.

## RESULTS AND DISCUSSIONS

### Synthesis of niosomes by batch and continuous approaches.

The most widely used method to produce niosomes is based on the thin-film hydration method where the surfactants and additives such as cholesterol are dissolved in an organic sol-

vent in a round bottom flask. Then, a thin film is formed on the inside wall of the flask by removing the organic solvent using a rotary vacuum evaporator. To form the niosomes, an aqueous/alcoholic solution is then added and the dry film is hydrated above the transition temperature ( $T_c$ ) of the surfactant, obtaining a white suspension (Figure 2-a). Dynamic light scattering of niosomes produced in the batch reactor, using the thin-film hydration method by the assistance of a highly energetic homogenization technique such as probe sonication at 60°C, rendered vesicles of  $339 \pm 42$  nm with a polydispersity index (PDI) of 0.137 and a zeta-potential of  $-75 \pm 7$  mV (Table 1). The PDI  $< 0.2$  indicates that the distribution consisted of a single size mode without showing aggregates. This high Zeta-potential value is in agreement with the literature<sup>26</sup> and ensures that the vesicles will repel each other and resist aggregation. In order to gain information concerning the morphology of the niosomes produced by the film hydration in batch, negative stained niosomes were analyzed by transmission electron microscopy as shown in Figure 2 a and b. TEM imaging of resulted niosomes evidenced the formation of round-shaped vesicles with a multilamellar structure formed by the assembly of hydrophobic and hydrophilic segments of the surfactant

Span 20, as it is depicted in Figure 1-c. The average diameter of the niosomes obtained from these images ( $187 \pm 55$  nm, Fig S1-a) is found to be well correlated with that obtained from DLS measurements. Although the size measurements determined by TEM are smaller than in DLS due to the lack of hydration. The production of niosomes by the film hydration method, but assisted by vortex instead of ultrasound is reported to render a heterogeneous particle-size distribution with a polydispersity index of 0.3.<sup>24</sup> This lack of control is due to a non-controlled shear stress to promote the proper assembly. Then, to suppress this limitation it is required the use of highly energetic homogenization techniques such as probe sonication. However, the sonication process presents a serious limitation for scaling-up the production of nanomaterials because the intensity of the ultrasound in a liquid decreases rapidly with the distance to the sonotrode.<sup>10</sup> It implies that larger volumes might not be well homogenized, providing a heterogeneous distribution of acoustic waves and consequent niosomes polydispersity.<sup>27</sup> In addition, it is reported that the cavitation generated during the ultrasonication process can etch the sonotrode tip surface, promoting a feasible product contamination with ions or particles from the sonotrode.<sup>27</sup> This phenomenon could be serious if the produced vesicles were aimed to be used in biomedical applications.

Considering that microfluidics enable a fast diffusion mixing by producing thin liquid lamellae,<sup>19</sup> we propose in this work to use a commercial slit-interdigital micromixer as a tool to assemble niosomes in a continuous flow (Figure 1-b). Lo et al.<sup>21</sup> reported the use of a hydrodynamic flow focusing microreactor to promote the fast self-assembly of niosomes and improve the control on their size distribution. This new approach was based on their procedure and the fast mixing achieved in the microchannels.<sup>21</sup> Niosomes were assembled by injecting the previously prepared thin film and dispersed in isopropyl alcohol into two adjacent PBS streams that enabled a hydrodynamical flow pattern.<sup>21</sup> Besides the excellent results achieved by Lo et al.<sup>21</sup>, the reactor throughput was very limited (100  $\mu$ l/min) and the microreactor was not commercially available with a limited access by non-microfluidic skilled users. As a contrary, the reactor proposed in this work is commercially available, enabling an easy reproduction of the reported results. In addition, the limited throughput was solved by a numbering-up approach, where 32 parallel microchannels were used

**Table 1.-Comparison of niosome characteristics prepared by different approaches in terms of size, polydispersity index and surface charge**

Synthesis approach	Niosome size DLS, (nm)	Polydispersity Index	Surface charge (mV)
Film hydration method   batch reactor	$339 \pm 42$	0.137	$-75 \pm 7$
Film hydration method   micro-mixer	$253 \pm 46$	0.156	$-35 \pm 1$
Emulsification   micro-mixer	$238 \pm 41$	0.135	$-33 \pm 3$

instead of the 3 channels used by Lo et al.<sup>21</sup>. The here proposed micromixer was previously applied by our group to successfully produce polymeric poly(lactic-co-glycolic acid) PLGA nanovesicles with a mean size of  $211 \pm 62$  nm.<sup>10</sup>

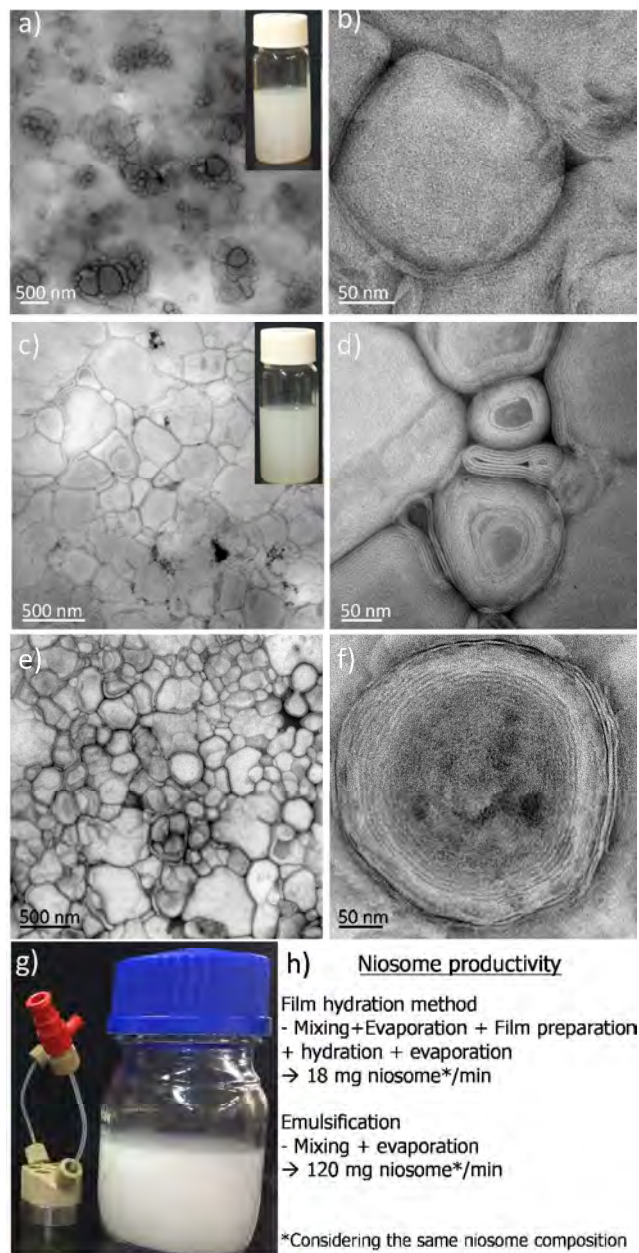


**Figure 2.-** TEM images of niosomes produced by different approaches. Thin film hydration method in batch reactor assisted by ultrasounds: (a) Overview of niosomes; (b) High magnification image of a multilamellar niosome. Thin film hydration method in a microfluidic mixer: (c) Overview of niosomes; (d) High magnification images of multilamellar niosomes. A compressed niosome is depicted, highlighting the high deformability index of this type of vesicles. Emulsification method in a microfluidic mixer, residence time = 10 ms,  $T^a = 55$  °C): (e) overview of niosomes; (f) High magnification image, observing the multilayer of SPAN and cholesterol over the whole particle. (g) Production of niosomes by the emulsification method with a micromixer (collecting time 90 s). (h) Comparison of niosome productivity between the film hydration method and the emulsification approach.

Those PLGA nanovesicles were formed under a residence time as short as 10 ms and a total flow rate of 48 ml/min.<sup>10</sup>

In this work, the hydrated thin film was dispersed in isopropyl alcohol and was split in 16 streams by using a commercial slit-interdigital micromixer. On the other hand, an aqueous stream was equally diverged into 16 slits, flowing thin aqueous laminated streams into the isopropyl alcohol streams and following a 90° trajectory to accelerate the mixing of miscible streams. The narrow width of the focused streams enables rapid mixing through diffusion. The mixing time ( $\tau_{mix}$ ) can be estimated for hydrodynamic flow focusing using a two-dimensional model as Equation 1.<sup>28</sup>

$$\text{Equation. 1} \quad \tau_{mix} \approx \frac{w^2}{9D} \cdot \frac{1}{(1 + FRR)^2}$$

where D is diffusivity of the solvent ( $10^{-9} \text{ m}^2 \cdot \text{s}^{-1}$ ), w is the microchannel width, and FRR is the ratio of flow rate of the water to isopropyl alcohol. It was observed that the increase of FRR from 15 to 50 resulted in a narrow niosome size distribution.<sup>21</sup> Consequently, the total volumetric flow rate, at a constant FRR (FRR= 50), was modified in the slit-interdigital micromixer to study whether a change in the residence time can enhance the diffusion mixing and render homogenous sized niosomes with a high production throughput. The total volumetric flow ratio was tuned from 0.48 ml/min to 48 ml/min, ranging the resulting residence time ( $t_m$ ) from 1 s to 0.01s, respectively. Considering that the  $\tau_{mix}$  (Equation 1) at a FRR = 50 was  $8 \cdot 10^{-2}$  ms, the range of total flow rates selected were large enough to promote the assembly of niosomes. Dynamic light scattering of produced niosomes elicited a reduction of mean particle size from  $2361 \pm 1109$  nm to  $253 \pm 46$  nm as the residence time was decreased from 1 s to 0.01 s, respectively. This result is in agreement with computational fluid dynamic analysis of the slit-interdigital micromixer used, where large flow rates promote a diffusive mixing enhancement that enables the production of nanovesicles instead of microvesicles.<sup>10</sup> Table 1 shows that the mean particle size achieved with the slit-interdigital micromixer at  $t_m = 0.01$ s ( $253 \pm 46$  nm) is smaller than that achieved with the batch-ultrasound assisted process. However, the PDI (PDI=0.156) of niosomes produced with the micromixer is slightly larger than the ones obtained with the batch-ultrasound assisted process, inferring from this result that the size distribution with the micromixer is less homogeneous.

Regarding the niosome surface charge produced with the micromixer, there is a sharp decrease in the Zeta-potential value, obtaining niosomes with a surface charge of  $-35 \pm 1$  mV. This difference can be associated with a lower inclusion of the charge inducing agent (DCP) in the lamellar structure. However the Zeta-potential value is higher than -30 mV and then, the colloidal niosomes are still stable for any desired biomedical use.<sup>12</sup> TEM images in Figure 2-c and d show that the morphology and lamellar structure is similar to the one achieved with the batch-ultrasound assisted process. The average diameter of the niosomes obtained from these images ( $298 \pm 49$  nm, Fig S1-b) is found to be well correlated with that obtained from DLS measurements. Considering that the synthesis of niosomes by the film hydration method is as semi-continuous procedure, the estimated productivity at the largest flow rate (48 ml/min) was 18 mg/min. Then, the productivity of niosomes is larger than the one achieved by Lo et al.<sup>21</sup> (100

$\mu\text{l}/\text{min}$ ), but it is still limited due to the multiple steps required to prepare the thin film composed by surfactant and additives. To face this shortcoming, we propose a novel strategy where the niosome reagents are injected in a single step at the micromixer and assembled by emulsification to render vesicles.

Two non-miscible streams were injected at the slit-interdigital micromixer to render a controlled emulsification process (Figure 1-b): 1) Organic stream. SPAN-20, DCP and cholesterol were dispersed in ethyl acetate and 2) Aqueous stream, composed of Milli-Q water. The reagent composition of the streams injected at the micromixer was similar to the one selected by the film hydration method, but using ethyl acetate instead of isopropyl alcohol. At the proper flow rates, the shear stress produced at the interphase of immiscible liquid microflows is energetic enough to promote the emulsion formation without the need of external mechanical or ultrasonic forces.<sup>10</sup> Finally, the organic solvent was evaporated to obtain the niosomes. This procedure is based on the well-known reverse phase evaporation technique, bypassing the time consuming operation of thin film-hydrated preparation, as well as enabling continuous niosome production.

Differently to reverse phase evaporation technique, the proposed procedure does not require vigorous conditions with high energetic sonication. Based on our previous work about the emulsification of poly(lactic-co-glycolic acid) PLGA with ethyl acetate and water as non-miscible solvents<sup>10</sup>, as well as the balance of high viscous shear stress and surface tension, emulsification of niosomes reagents was carried out at the highest flow rate achievable with the pumping setup (48 ml/min). This flow rate implies that the residence time of the injected reagents at the slit-interdigital micromixer was 10ms. Interestingly, the direct assembly of niosomes by emulsification rendered multi-lamellar niosomes with similar morphology and microstructure than the ones achieved by the film hydration method either in batch, assisted by ultrasounds, or in the micromixer (Figure 2 e-f). The average diameter of the niosomes obtained from these TEM images ( $181 \pm 39$  nm, Fig S1-c) was found to be well correlated with that obtained from DLS measurements. A detail TEM image with high magnification enables to resolve an onion-like organization of the niosome membrane (Figure 2-f). Dynamic light scattering unveiled that the size of produced niosomes ( $238 \pm 41$  nm) was smaller than those obtained with previous procedures. The PDI (0.135) was similar to the one achieved with sonication (0.137), inferring from this result that microfluidic technology is an alternative to high energetic procedures, but it leverages for the continuous, non-contaminated and controlled production. Regarding the surface charge of niosomes produced by emulsification, it is similar to the one produced by the film hydration method with the micromixer. Finally, the productivity achieved by the emulsification methods clearly overpasses the productivity of previous reported procedures, obtaining a throughput of 120 mg of niosomes/min.

#### Electronic microscopy characterization of niosome bilayers.

Considering that a detailed description of the niosomes structure by electron microscopy is scarce and there is a limited amount of available data, we aim to provide insight into their bilayer structure by imaging techniques. As far as we know, niosomes were never studied before using high resolution scanning transmission microscopy. Figure 3 shows STEM-HAADF images of negative stained niosomes produced by the

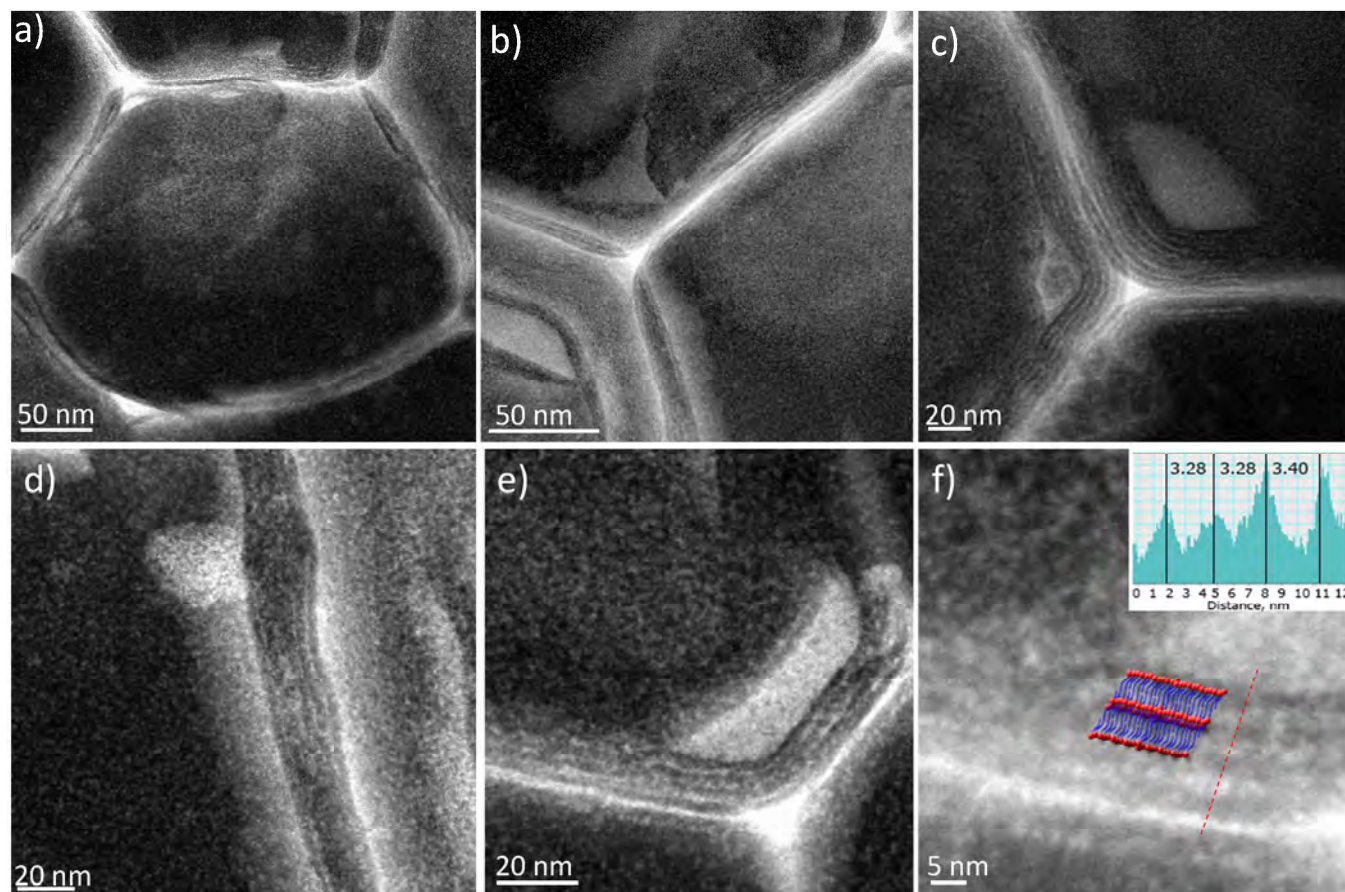


**Figure 3.-** STEM-HAADF images of the niosome nanostructure. The niosomes were produced using the emulsification process at a residence time of 10 ms and 55 °C. The niosomes were negatively stained with phosphotungstic acid: a) The collapsed structure of a niosome after drying. b) Magnification image to confirm the presence of a multilamellar shell and a hollow inner structure. c) Detail image of the bilayer shells of two contiguous niosomes. d-e) High resolution images of the niosome bilayer at different locations. f) High resolution image of niosome bilayers. Bilayer thickness determination by imaging profile (red dashed line) and interpretation of the Span 20/Cholesterol bilayer according to molecular simulations.<sup>29</sup>

emulsification method. The collapsed structure of the niosome after drying confirms the presence of a multi-lamellar shell of approx. 12 nm and a hollow structure (Figure 3 a-c). This result is in agreement with previous observations,<sup>22, 30</sup> where it is shown that niosomes are capable of encapsulating both hydrophilic and lipophilic substances. The hydrophilic molecules are entrapped in the vesicular aqueous core or adsorbed on the bilayer surfaces while the lipophilic substances are encapsulated into the lipophilic domain of the bilayers (Figure 1-c).<sup>22</sup> High resolution STEM-HAADF images elicited the microstructure of the niosome wall, evidencing the presence of 3 bilayers (Figure 3 d-e). The stability of the bilayers as well as their rigidity are essentially governed by the hydrogen bonding between the ester group of Span20 and hydroxyl group of cholesterol.<sup>31</sup> According to Figure 3-f, the estimated dimension of each bilayer is  $3.35 \pm 0.15$  nm and it is in agreement with molecular simulations<sup>29</sup> and experimental data where the area per molecule of Span 20 is approximately  $22 \text{ \AA}^2$ .<sup>32</sup> This result is also in agreement with the thickness of some reported bilayers: 1) 4.18 nm,<sup>29</sup> composed of Span 60 and cholesterol, 2) 3.49 nm,<sup>29, 33</sup> composed of Span 80 and cholesterol and 3) 3.53 nm,<sup>33</sup> composed of DOPC (1,2-dioleoyl-sn-glycero-3-phosphocholine) and cholesterol.

#### Effect of hydration temperature on niosomes.

One of the important parameters that has a direct effect on the niosome formation is the processing temperature.<sup>22</sup> The hydration temperature used to produce niosomes should usually be above the gel to liquid phase transition temperature ( $T_c$ ) of the surfactant. Considering that the  $T_c$  of Span-20 is 16 °C,<sup>34</sup> we have studied the influence of the processing temperature during the emulsification process at a range of temperatures > 16°C. Figure 4 depicts the TEM images of resulting niosomes obtained at mixing temperatures of 25, 35, 45 and 55 °C. TEM images reveals that niosomes are produced in all the range of temperature tested. Their morphology is similar in all conditions, obtaining a multi-lamellar structure. However, the dimension of the niosomes is sensitive to the hydration temperature, observing larger niosomes as the temperature was increased. Particle-size distribution histograms resulted from TEM images analysis (Fig. S2) show that the mean niosome sizes were:  $108 \pm 24$  nm at 25 °C,  $201 \pm 43$  nm at 35°C,  $232 \pm 39$  nm at 45°C, and  $228 \pm 39$  nm at 55 °C. Dynamic light scattering of the produced niosomes elicited the TEM observed tendency:  $224.0 \pm 25.5$  nm at 25 °C,  $255.7 \pm 28.2$  nm at 35 °C,  $284.3 \pm 37.0$  nm at 45 °C and  $361.7 \pm 38.2$  nm at 55 °C. On the other hand, the surface charge was similar in all of them with a mean value of  $-38.9 \pm 6.3$  mV. The results observed are in agreement with previous results where the effect



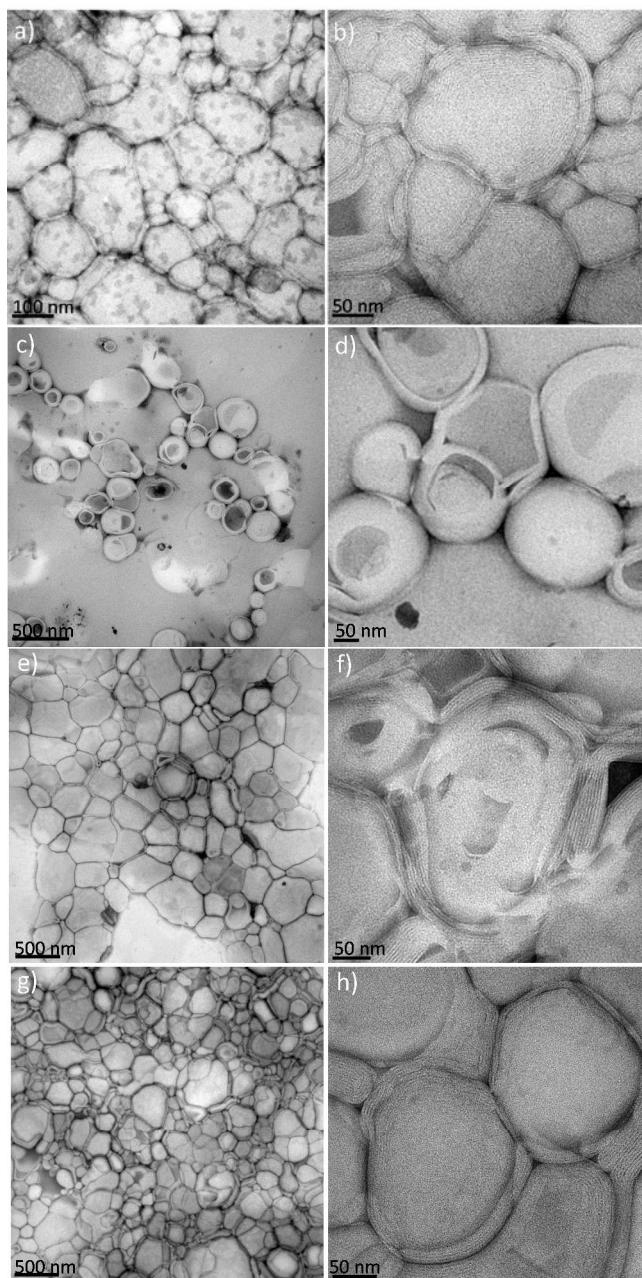


**Figure 4.-** Effect of hydration temperature on niosomes. TEM images showing niosomes synthesized by the emulsification technique, under temperature changes of the aqueous phase. Low magnification images to observe the niosome size distribution and high magnification images where the bilayer structure is depicted of niosomes produced at: (a-b) 25 °C; (c-d) 35 °C; (e-f) 45 °C; (f-g) 55 °C.

of temperature on sorbitan surfactant monolayers was observed.<sup>32</sup> Generally, as the temperature is increased, the collapse temperature of surfactant Span-20, Span 40 and Span 60 is lowered, inferring from this fact that the films were more expanded as the temperature was increased.<sup>32</sup>

Consequently, it seems coherent that a more expanded structure can give rise to larger niosomes. This evidenced that the hydration temperature is one of the key factors to control the size of niosomes. In addition, and considering that the final application of niosomes is intended for a biomedical use, the

layers produced at a high temperature are less stable than the ones produced at low temperatures (over the  $T_c$ ).<sup>32</sup>

#### Study of niosome stability.

Niosomes stability was assessed by monitoring changes in size for the resulting vesicles over time, to predict their swelling, degradation or potential aggregation characteristics. Hydrated bilayers of niosomes are not considered to be thermodynamically stable<sup>35</sup>, and then, niosomes can exhibit changes during long-term storage. To investigate the stability of the niosomes, they were dispersed in PBS and stored in glass vials at room temperature and in the refrigerator (4 °C), for a period of 6 weeks. The hydration media has a key effect on niosome stability<sup>26</sup>, being more stable in aqueous media than in saline solutions<sup>36</sup>. Niosomes were dispersed in PBS in order to test the most comparable conditions to a physiological media for the hydrated bilayers. For niosomes prepared with microfluidic reactors by the emulsification and film hydration method, the particle size showed a decrease in the first week, and then remained stable throughout the study when niosomes were indifferently stored at 25°C or at 4°C (Figure 5-a). Niosomes produced by the emulsification method underwent a 30% size reduction rate during the first week of storage, whereas niosomes produced by the film hydration method exhibited a 20% size reduction.

The size reduction can be directly related with the osmotic pressure through the niosome bilayers. This phenomenon has been previously observed in liposomes, where a saline solution exposure reduces the dimension with a size variation ratio of up to 0.2 in response to osmotic forces<sup>37, 38</sup>. The shrinkage in liposomes size was also previously observed during an initial period of time (12h) and then, no size variations were observed<sup>37, 38</sup>. The reduction in niosome size also causes the hydrated bilayers to compress and this could affect their stability. TEM images depicted in Figure 5 also confirm the reduction in size for both emulsification (61 and 44 nm for cold and room temperature storage, respectively) and film hydrated (72 and 71 nm for cold and room temperature storage, respectively) approaches. However, the structure of hydrated bilayers after 6 weeks in PBS was still stable and a multi-lamellar shell of approximately 12 nm was observed. This result is coherent with the previous literature where the presence of DCP and cholesterol improved the physicochemical properties of niosomes and assured their bilayer stability<sup>4</sup>. On the other hand, there were no significant changes in the surface charge of niosomes regardless of the storage temperature. This fact is in agreement with the aforementioned bilayer stability and the physicochemical role of DCP and cholesterol.

On the other hand, the stability of niosomes produced by the emulsification method in the microfluidic system were studied in DMEM as culture media. As can be inferred from Table S1, no significant changes in particle size were observed after three weeks. DMEM is a high glucose culture medium supplemented with 10% fetal bovine serum that promotes the niosome stabilization probably because a protein corona is surrounding the surface of the niosomes and avoids any size reduction.

Niosome formulations are preferred to be stored at low temperature because the retention of encapsulated active biomolecules or drugs is diminished as the storage temperature is increased<sup>39</sup>. This fact is due to the degradation of surfactants in the bilayers, resulting in defects in the membrane packing<sup>40</sup>.

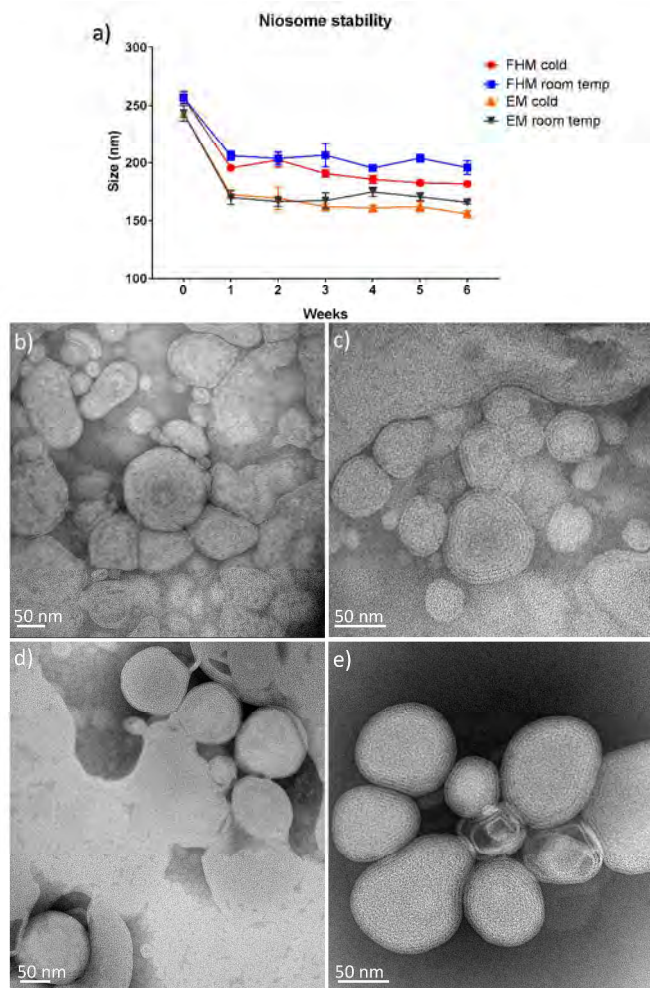


**Figure 5.-** Stability of niosomes prepared by emulsification (residence time of 10 ms and 55 °C) and film hydration, using PBS as hydration media and a stored temperature of 4 °C and 25 °C. The data represents the mean  $\pm$  SD measured by DLS. TEM images of niosomes stored during 6 weeks with PBS; niosomes synthesized by the film hydration method using microfluidics, stored at: b) 25 °C, c) 4 °C. Niosomes synthesized by emulsification, stored at: d) 25 °C, e) 4 °C

To address this lack of retention control, niosomes are usually lyophilized either with a cryoprotectant such as mannitol<sup>41</sup> or even just without a cryoprotectant<sup>39</sup>. Figure 6 depicts the niosomes produced after lyophilizing by freezing the niosome dispersion at  $-70$  °C and drying under vacuum for 24 hours. Lyophilized niosomes tended to assembly into short chains of approx. 500 nm in diameter and few vesicles length. The vesicles still kept the niosome bilayer structure as it is depicted in Figure 6-b. The niosome assembly was also produced if a cryoprotectant were also used (Figures 6-c,d). These results imply that niosome could fuse during the lyophilization conditions to generate niosome assemblies. This phenomenon was previously reported to enhance the drug loading in niosomes<sup>34</sup>, but no electronic imaging evidences were provided to support this niosomal fusion. The same mechanism was also reported by Ohsawa et al.<sup>42</sup>, using the well-known freeze-drying method to enhance the encapsulation of biomolecules and drugs in liposomes. The mechanism explained to promote the encapsulation during the freeze thawing cycle is based on<sup>34, 39</sup>: 1) the drug and vesicles are concentrated while freezing, 2) vesicles

were closely packed with each other resulting in their fusion 3) new vesicles are formed, enhancing the efficient entrapment of drugs or active biomolecules.

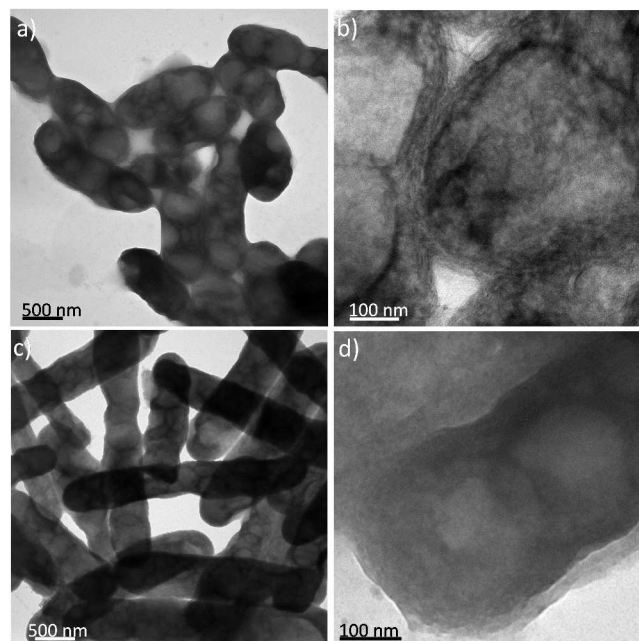


**Figure 6.-**TEM images of lyophilized niosomes produced by emulsification at a residence time of 10 ms and 55 °C: a-b) without cryoprotectant; c-d)with mannitol (2.5 wt.%) as cryoprotectant.

#### Cytotoxicity studies

The cytocompatibility of the synthesized niosomes (0.01-0.4 mg/mL) from both methodologies was assessed in three cell lines related to skin (human dermal fibroblasts, keratinocytes and macrophages), due not only to their potential cosmetic use but also to their feasible dermal and transdermal delivery of compounds with therapeutic or diagnostic purposes. Figure 7 depicts the viability percentages estimated by the Alamar Blue assay after incubation for 24 h of the cell types assayed with niosomes obtained from TFH methodology (Figure 7a) and emulsification (Figure 7b). In both cases, viability was always higher than 70%, which is the minimum concentration recommended of the ISO 10993-5<sup>43</sup> for these types of materials in which viabilities higher than 70% are considered cytocompatible. Specifically, fibroblasts displayed percentages around or higher than 90% while keratinocytes reached values between 95-100%, pointing to the high cytocompatibility of the niosomes tested. On the other hand, macrophages showed a decrease in viability with the increase in niosomes concentration up to 65-70% at the highest concentration assayed (0.4 mg/mL), which may be related to the phagocytic role of this cell line<sup>44</sup>.

Even though little is known about niosomes cytotoxicity, previous studies have also shown the high cytocompatibility of niosomes containing Span 60 in human lung carcinoma cells but at much lower concentrations than ours ( $\leq 12$   $\mu\text{g/mL}$ )<sup>45</sup>. Other authors have also used Span 20-niosomes with transfection purposes showing successful results in HeLa cells<sup>46</sup> or even with anti-inflammatory purposes in NCTC2544 human keratinocytes pointing to not significant mortality percentages up to a concentration of 1  $\mu\text{M}$  when Tween 85 was the surfactant used<sup>47</sup>. Taken together these studies and our observations,

niosomes appear as a good tool for novel biomedical strategies.

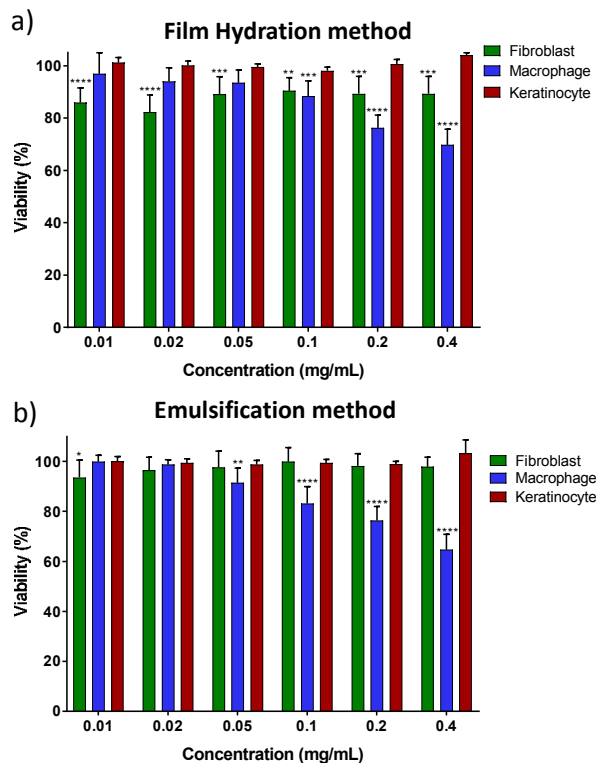


**Figure 7.-** Cell viability of fibroblasts, macrophages and keratinocytes in the presence of 0.01-0.4mg/mL of niosomes after 24 hours incubation following: (a) the film hydration method and (b) the emulsification method.

#### Co-encapsulation of model fluorescent molecules.

Lamellarity was also qualitatively assessed using confocal laser scanning microscopy (CLSM) in order to use the produced niosomes for a potential dual drug delivery application. The preferential distribution of hydrophobic (Nile red) and hydrophilic (sodium fluorescein) model fluorescent molecules within niosomes was investigated. As it is depicted in Figure 1-c, Nile red should be selectively attached to the tail group of Span 20 amphiphilic bilayers; whereas fluorescein should be located at the hydrophilic niosome core close to the hydrophilic head group of Span 20. CLSM visualization of single niosomes was not possible due to the reduced resolution of this imaging technique (i.e., <200nm). However the analysis of fused niosomes unveiled that the hydrophobic and hydrophilic dyes were successfully loaded in the same vesicle (Figure 8 a,b). Figure 8-c depicts the overlapped image of loaded dyes to show the uniform encapsulation at the core and at the shell. The bright green spots located at the shell are believed to be aggregates of single niosomes (Figure 8-d), where the hydrophilic core has a brighter emission than the one produced by the few hydrophobic bilayers (10-15 nm) where Nile red is entrapped. These results are in agreement with previously reported results<sup>36</sup> based on the dual encapsulation by the film hydration method, and confirm that hydrophilic and hydrophobic groups of Span20 could be successfully used to simultaneously encapsulate hydrophobic and hydrophilic drugs. Consequently, the simultaneous encapsulation of molecules of different polarity here demonstrated

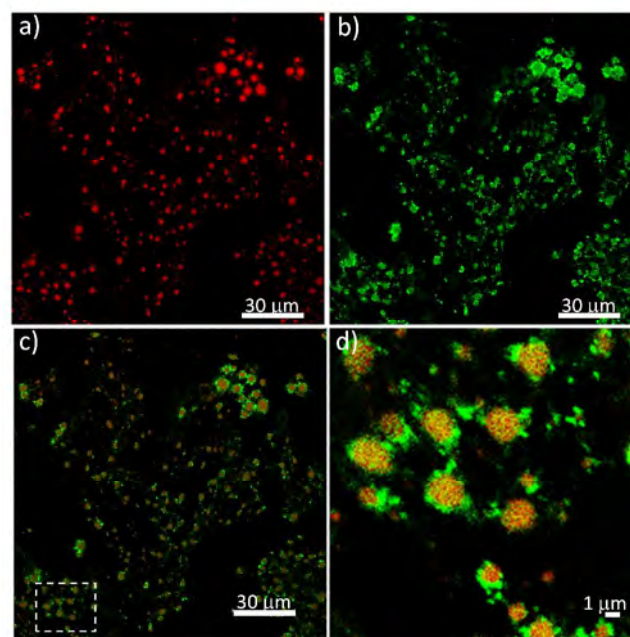


**Figure 8.-** Encapsulation of Nile red and sodium fluorescein in niosomes produced by the emulsification method at a residence time of 10 ms and 55°C: (a) red channel (Nile red) (b) green channel (sodium fluorescein), and (c) overlapped image of red and green channels, (d) high magnification image of overlapped red and green channels of the area marked in (c).

might be extended to the co-administration of drugs of different nature overcoming the associate limitations of drug solubility and also favoring the potential synergistic action of different drugs contained in the same carrier. In addition, it is well known that the stratum corneum is largely hydrophobic and the use of a carrier able to deliver transdermally hydrophilic drugs represents a clear advantage of niosomes as carriers in topical delivery

## CONCLUSIONS

HRTEM, confocal microscopy and dynamic light scattering analyses have corroborated the successful synthesis of niosomes in a continuous manner with high particle monodispersity. Compared to the traditional batch process the microfluidic synthesis here reported produces much more yield in shorter periods of time with enhanced monodispersity. The subcytotoxic doses on three different somatic cell lines have been evaluated displaying high cytocompatibility even at the highest doses tested. Aging and freeze-drying effects have been evaluated on the resulting niosomes. The niosomes here described are able to carry both hydrophilic and hydrophobic molecules highlighting their potential application as dual drug delivery carriers.

## ASSOCIATED CONTENT

**Supporting Information.** Supplementary information and figures are included. This material is available free of charge via the Internet at <http://pubs.acs.org>. For instructions on what should be included in the Supporting Information as well as how to prepare this material for publication, refer to the journal's Instructions for Authors.

## AUTHOR INFORMATION

### Corresponding Author

\* arruebom@unizar.es, victorse@unizar.es.

### ACKNOWLEDGMENT

The authors gratefully acknowledge the financial support of the ERC Consolidator Grant program (ERC-2013-CoG-614715, NANOHEDONISM). CIBER-BBN is an initiative funded by the VI National R&D&I Plan 2008–2011, Iniciativa Ingenio 2010, Consolider Program, CIBER Actions and financed by the Instituto de Salud Carlos III (Spain) with assistance from the European Regional Development Fund.

### REFERENCES

- Capretto, L.; Carugo, D.; Mazzitelli, S.; Nastruzzi, C.; Zhang, X. L., Microfluidic and lab-on-a-chip preparation routes for organic nanoparticles and vesicular systems for nanomedicine applications. *Adv Drug Deliver Rev* **2013**, 65, (11-12), 1496-1532.
- Albisa, A.; Espanol, L.; Prieto, M.; Sebastian, V., Polymeric Nanomaterials as Nanomembrane Entities for Biomolecule and Drug Delivery. *Curr Pharm Design* **2017**, 23, (2), 263-280.
- Kuchler-Bopp, S.; Larrea, A.; Petry, L.; Idoux-Gillet, Y.; Sebastian, V.; Ferrandon, A.; Schwinté, P.; Arruebo, M.; Benkirane-Jessel, N., Promoting bioengineered tooth innervation using nanostructured and hybrid scaffolds. *Acta Biomaterialia* **2017**, 50, 493-501.
- Basiri, L.; Rajabzadeh, G.; Bostan, A.,  $\alpha$ -Tocopherol-loaded niosome prepared by heating method and its release behavior. *Food Chemistry* **2017**, 221, 620-628.
- Espanol, L.; Larrea, A.; Andreu, V.; Mendoza, G.; Arruebo, M.; Sebastian, V.; Aurora-Prado, M. S.; Kedor-Hackmann, E. R. M.; Santoro, M. I. R. M.; Santamaria, J., Dual encapsulation of hydrophobic and hydrophilic drugs in PLGA nanoparticles by a single-step method: drug delivery and cytotoxicity assays. *Rsc Adv* **2016**, 6, (112), 111060-111069.
- Trotta, M.; Gallarate, M.; Pattarino, F.; Morel, S., Emulsions containing partially water-miscible solvents for the preparation of drug nanosuspensions. *J Control Release* **2001**, 76, (1-2), 119-128.
- Chew, J. W.; Black, S. N.; Chow, P. S.; Tan, R. B. H., Comparison between open-loop temperature control and closed-loop supersaturation control for cooling crystallization of glycine. *Ind Eng Chem Res* **2007**, 46, (3), 830-838.
- Albisa, A.; Piacentini, E.; Sebastian, V.; Arruebo, M.; Santamaria, J.; Giorno, L., Preparation of Drug-Loaded PLGA-PEG Nanoparticles by Membrane-Assisted Nanoprecipitation. *Pharmaceutical Research* **2017**, 1-13.
- Peer, D.; Karp, J. M.; Hong, S.; FaroKHzad, O. C.; Margalit, R.; Langer, R., Nanocarriers as an emerging platform for cancer therapy. *Nat Nanotechnol* **2007**, 2, (12), 751-760.
- de Solorzano, I. O.; Uson, L.; Larrea, A.; Miana, M.; Sebastian, V.; Arruebo, M., Continuous synthesis of drug-loaded nanoparticles using microchannel emulsification and numerical modeling: effect of passive mixing. *Int J Nanomed* **2016**, 11, 3397-3416.
- Sebastian, V.; Arruebo, M.; Santamaria, J., Reaction Engineering Strategies for the Production of Inorganic Nanomaterials. *Small* **2014**, 10, (5), 835-853.
- Marianecci, C.; Di Marzio, L.; Rinaldi, F.; Celia, C.; Paolino, D.; Alhaique, F.; Esposito, S.; Carafa, M., Niosomes from 80s to present: The state of the art. *Adv Colloid Interfac* **2014**, 205, 187-206.
- Uchehgbu, I. F.; Vyas, S. P., Non-ionic surfactant based vesicles (niosomes) in drug delivery (vol 172, pg 33, 1998). *Int J Pharm* **1998**, 176, (1), 139-139.
- Manconi, M.; Vila, A. O.; Sinico, C.; Figueruelo, J.; Molina, F.; Fadda, A. M., Theoretical and experimental evaluation of decypolyglucoside vesicles as potential drug delivery systems. *J Drug Deliv Sci Tec* **2006**, 16, (2), 141-146.
- Kazi, K. M.; Mandal, A. S.; Biswas, N.; Guha, A.; Chatterjee, S.; Behera, M.; Kuotsu, K., Niosome: A future of targeted drug delivery systems. *J Adv Pharm Technol Res* **2010**, 1, (4), 374-380.
- Roy, A.; Pyne, A.; Pal, P.; Dhara, S.; Sarkar, N., Effect of Vitamin E and a Long-Chain Alcohol n-Octanol on the Carbohydrate-Based Nonionic Amphiphile Sucrose Monolaurate—Formulation of Newly Developed Niosomes and Application in Cell Imaging. *ACS Omega* **2017**, 2, (11), 7637-7646.
- Roy, A.; Kundu, N.; Banik, D.; Sarkar, N., Comparative Fluorescence Resonance Energy-Transfer Study in Pluronic Triblock Copolymer Micelle and Niosome Composed of Biological Component Cholesterol: An Investigation of Effect of Cholesterol and Sucrose on the FRET Parameters. *J Phys Chem B* **2016**, 120, (1), 131-142.
- Kitaoka, M.; Goto, M., Transcutaneous Immunization Using Nano-sized Drug Carriers. Zheng-Rong Lu and Shinji Sakuma (eds.), Springer Science+Business Media New York 2016. *Nanomaterials in Pharmacology*, **2015**; 349-367.
- Marre, S.; Jensen, K. F., Synthesis of micro and nanostructures in microfluidic systems. *Chem Soc Rev* **2010**, 39, (3), 1183-1202.
- Amoabediny, G.; Haghirsadat, F.; Naderinezhad, S.; Helder, M. N.; Akhondi Kharanaghi, E.; Mohammadnejad Arough, J.; Zandieh-Doulabi, B., Overview of preparation methods of polymeric and lipid-based (niosome, solid lipid, liposome) nanoparticles: A comprehensive review. *International Journal of Polymeric Materials and Polymeric Biomaterials* **2018**, 67, (6), 383-400.
- Lo, C. T.; Jahn, A.; Locascio, L. E.; Vreeland, W. N., Controlled Self-Assembly of Monodisperse Niosomes by Microfluidic Hydrodynamic Focusing. *Langmuir* **2010**, 26, (11), 8559-8566.
- Moghassemi, S.; Hadjizadeh, A., Nano-niosomes as nanoscale drug delivery systems: An illustrated review. *J Control Release* **2014**, 185, 22-36.
- Obeid, M. A.; Gebril, A. M.; Tate, R. J.; Mullen, A. B.; Ferro, V. A., Comparison of the physical characteristics of monodisperse non-ionic surfactant vesicles (NISV) prepared using different manufacturing methods. *Int J Pharm* **2017**, 521, (1-2), 54-60.
- Paolino, D.; Cosco, D.; Muzzalupo, R.; Trapasso, E.; Picci, N.; Fresta, M., Innovative bola-surfactant niosomes as topical delivery systems of 5-fluorouracil for the treatment of skin cancer. *Int J Pharm* **2008**, 353, (1-2), 233-242.
- Murphy, C. J.; Buriak, J. M., Best Practices for the Reporting of Colloidal Inorganic Nanomaterials. *Chemistry of Materials* **2015**, 27, (14), 4911-4913
- Obeid, M. A.; Khadra, I.; Mullen, A. B.; Tate, R. J.; Ferro, V. A., The effects of hydration media on the characteristics of non-ionic surfactant vesicles (NISV) prepared by microfluidics. *Int J Pharm* **2017**, 516, (1), 52-60.
- Larrea, A.; Clemente, A.; Luque-Michel, E.; Sebastian, V., Efficient production of hybrid bio-nanomaterials by continuous microchannel emulsification: Dye-doped SiO<sub>2</sub> and Au-PLGA nanoparticles. *Chemical Engineering Journal* **2017**, 316, (Supplement C), 663-672.
- Karnik, R.; Gu, F.; Basto, P.; Cannizzaro, C.; Dean, L.; Kyei-Manu, W.; Langer, R.; Farokhzad, O. C., Microfluidic platform for controlled synthesis of polymeric nanoparticles. *Nano Lett* **2008**, 8, (9), 2906-2912.
- Ritwiset, A.; Kongsuk, S.; Johns, J. R., Molecular structure and dynamical properties of niosome bilayers with and without cholesterol incorporation: A molecular dynamics simulation study. *Applied Surface Science* **2016**, 380, (Supplement C), 23-31.
- Mandal, S.; Banerjee, C.; Ghosh, S.; Kuchlyan, J.; Sarkar, N., Modulation of the Photophysical Properties of Curcumin in Nonionic Surfactant (Tween-20) Forming Micelles and Niosomes: A Comparative Study of Different

- Microenvironments. *The Journal of Physical Chemistry B* **2013**, 117, (23), 6957-6968.
- (31) Nasser, B., Effect of cholesterol and temperature on the elastic properties of niosomal membranes. *Int J Pharm* **2005**, 300, (1), 95-101.
- (32) Peltonen, L.; Hirvonen, J.; Yliruusi, J., The Effect of Temperature on Sorbitan Surfactant Monolayers. *Journal of Colloid and Interface Science* **2001**, 239, (1), 134-138.
- (33) Han, S., Molecular Dynamics Simulation of Sorbitan Monooleate Bilayers. ed.; 2013; Vol. 34. No. 3, 946-947
- (34) Mokhtar, M.; Sammour, O. A.; Hammad, M. A.; Megrab, N. A., Effect of some formulation parameters on flurbiprofen encapsulation and release rates of niosomes prepared from proniosomes. *Int J Pharm* **2008**, 361, (1), 104-111.
- (35) Basiri, L.; Rajabzadeh, G.; Bostan, A.,  $\alpha$ -Tocopherol-loaded niosome prepared by heating method and its release behavior. *Food Chemistry* **2017**, 221, (Supplement C), 620-628.
- (36) Sharma, V.; Anandhakumar, S.; Sasidharan, M., Self-degrading niosomes for encapsulation of hydrophilic and hydrophobic drugs: An efficient carrier for cancer multi-drug delivery. *Materials Science and Engineering: C* **2015**, 56, (Supplement C), 393-400.
- (37) Pencer, J.; White, G. F.; Hallett, F. R., Osmotically induced shape changes of large unilamellar vesicles measured by dynamic light scattering. *Biophysical Journal* **2001**, 81, (5), 2716-2728.
- (38) Wolfram, J.; Suri, K.; Yang, Y.; Shen, J.; Celia, C.; Fresta, M.; Zhao, Y.; Shen, H.; Ferrari, M., Shrinkage of pegylated and non-pegylated liposomes in serum. *Colloids and surfaces. B, Biointerfaces* **2014**, 114, 294-300.
- (39) Arafa, M. G.; Ayoub, B. M., DOE Optimization of Nano-based Carrier of Pregabalin as Hydrogel: New Therapeutic & Chemometric Approaches for Controlled Drug Delivery Systems. *Sci Rep-Uk* **2017**, 7. Article number 41503.
- (40) Biswal, S.; Pn, M.; Sahu, J.; Sahoo, P.; Amir, F., *Vesicles of Non-ionic Surfactants (Niosomes) and Drug Delivery Potential.*; *Int. J. Pharm. Sci. Nanotech* **2008**; 1,1-7
- (41) Bhaskaran, S.; K. Lakshmi, P., Comparative evaluation of niosome formulations prepared by different techniques. ed.; *Acta Pharm Sci* **2009**; 51, 27-32.
- (42) Ohsawa, T.; Miura, H.; Harada, K., A Novel Method for Preparing Liposome with a High-Capacity to Encapsulate Proteinous Drugs - Freeze-Drying Method. *Chem Pharm Bull* **1984**, 32, (6), 2442-2445.
- (43) Part 5: Tests for in vitro cytotoxicity ISO 10993-5:2009 - Biological evaluation of medical devices-  
[http://www.iso.org/iso/catalogue\\_detail.htm?csnumber=36406](http://www.iso.org/iso/catalogue_detail.htm?csnumber=36406).  
(1/February/2018),
- (44) Aderem, A.; Underhill, D. M., Mechanisms of phagocytosis in macrophages. *Annu Rev Immunol* **1999**, 17, 593-623.
- (45) Asthana, G. S.; Sharma, P. K.; Asthana, A., In Vitro and In Vivo Evaluation of Niosomal Formulation for Controlled Delivery of Clarithromycin. *Scientifica* **2016**. Article number 6492953.
- (46) Paecharoenchai, O.; Niyomtham, N.; Ngawhirunpat, T.; Rojanarata, T.; Yingyongnarongkul, B. E.; Opanasopit, P., Cationic niosomes composed of spermine-based cationic lipids mediate high gene transfection efficiency. *J Drug Target* **2012**, 20, (9), 783-792.
- (47) Marianecchi, C.; Rinaldi, F.; Matriota, M.; Pieretti, S.; Trapasso, E.; Paolino, D.; Carafa, M., Anti-inflammatory activity of novel ammonium glycyrrhizinate/niosomes delivery system: Human and murine models. *J Control Release* **2012**, 164, (1), 17-25.

Insert Table of Contents artwork here



1  
2  
3  
4  
5  
6  
7  
8  
9  
10  
11  
12  
13  
14  
15  
16  
17  
18  
19  
20  
21  
22  
23  
24  
25  
26  
27  
28  
29  
30  
31  
32  
33  
34  
35  
36  
37  
38  
39  
40  
41  
42  
43  
44  
45  
46  
47  
48  
49  
50  
51  
52  
53  
54  
55  
56  
57  
58  
59  
60